$_5$wt increased, whereas b $_5$ext decreased, the relative contribution to the total enthalpy of the higher temperature, phase-separated component. These results were con rmed with uorescence measurements by using pyrene-labeled phospholipids. The dissimilar interaction with lipids of these two differently localized TA proteins could have implications for their intracellular sorting.

cytochrome b $_5$ differential scanning calorimetry endoplasmic reticulum lipid domains liposomes

At the interface between the endoplasmic reticulum (ER) and the Golgi complex, sophisticated mechanisms operate to sort proteins destined for export from those that remain ER residents. The operation of these mechanisms depends on amino acid sequences within exported and nonexported proteins that mediate the molecular interactions involved in sorting. Over the past years, much progress has been made in describing the interactions between these sequences and protein components of the sorting machinery (reviewed in ref. 1). In addition to protein–protein recognition events, however, protein–lipid interactions involving the transmembrane domain (TMD) of integral membrane proteins and bilayer lipids may be important.

Membranes of different intracellular compartments have different lipid compositions that result in a gradient of increasing thickness and decreasing fluidity of the bilayer down the secretory pathway (2–4). Because glycerophospholids and sphingolipids are initially synthesized in the ER, these intercompartmental differences must be generated by subsequent remodeling and or by specific lipid transfer between compartments. The latter process is likely to be effected by more than one mechanism, but lipid sorting during formation of transport vesicles is thought to play an important role (4–6). This process involves lateral segregation of lipids in the bilayer plane with formation of domains and might result in the differential sorting of membrane proteins on the basis of their partitioning into these domains. Such a mechanism has indeed been implicated in the retention of Golgi enzymes (2) and in apical sorting of membrane proteins in epithelial cells (7, 8). Moreover, in yeast, export of glycosylphosphatidylinositol-anchored proteins from the ER is linked to ceramide synthesis, suggesting that export of this lipid and GPI-anchored proteins are coupled events (9). However, in mammalian cells evidence for participation of lipids in sorting at the ER Golgi interface is lacking so far.

A number of proteins depend on features in their TMD for correct sorting at the ER Golgi interface. In particular, C-tail anchored (TA) proteins often require a short and moderately hydrophobic TMD to remain residents of the ER, and they have provided useful models for the study of the role of the TMD in sorting at the earliest steps of the secretory pathway (reviewed in ref. 10). In some cases, TMD-dependent sorting is mediated by a proteinaceous receptor, rer1p, which binds ER residents that have escaped to the Golgi complex and returns them to the ER (11). Other TMD-dependent proteins, however, do not depend on rer1p-mediated retrieval for their ER residency (12) and are thus candidates for lipid-dependent sorting.

Here, we have used differential scanning calorimetry (DSC) to investigate in a membrane-mimicking system a possible role of lipids in the TMD-dependent sorting of TA proteins at the ER Golgi interface. DSC is used to monitor the thermotropic properties (gel-liquid transition temperature, T_m, and enthalpy,) of lipid bilayers, providing information on the existence of lipid lateral phase separation and on the interactions of proteins with these domains (13, 14). As model proteins, we have chosen the ER resident TA protein cytochrome b_5 ($b_5$wt) and a mutant version thereof, $b_5$ext, that in vivo is transported to the plasma membrane because of the presence of five additional hydrophobic residues in its TMD (15). The two proteins have been incorporated into liposomes constituted by a matrix of palmitoyl-oleyl-phosphatidylcholine (POPC), a ubiquitous and low-temperature melting lipid, mixed with a higher-temperature melting component, i.e., a glycerophospholipid with different

Con ict of interest statement: No con icts declared.

Abbreviations: CER, C16-ceramide; DSC, differential scanning calorimetry; DSPC, distearoylphosphatidylcholine; DSPS, distearoyl phosphatidylserine; ER, endoplasmic reticulum; OG, N-octyl glucoside; POPC, palmitoyl-oleyl-phosphatidylcholine; POPS, palmitoyl-oleyl-phosphatidylserine; PS, phosphatidylserine; pyrene-PC, 1-palmitoyl-2-(1-pyrenedecanoyl)-sn-glycerol-3-phosphocholine; pyrene-PS, 1-palmitoyl-2-(1-pyrenedecanoyl)-sn-glycerol-3-phosphoserine; TA, tail-anchored; T_m, gel-liquid transition temperature; TMD, transmembrane domain.

§N.B. and M.M. contributed equally to this work.

¶To whom correspondence may be addressed. E-mail: n.borgese@in.cnr.it or massimo.masserini@unimib.it.

acyl chains and/or headgroup, or C16-ceramide (CER). We find that $b_5$wt and $b_5$ext have distinctly different behavior with respect to the domains that these lipids form in POPC bilayers. Our results are consistent with the idea that the TMD-dependent sorting of TA proteins at the ER/Golgi interface may involve the exclusion of a short, moderately hydrophobic TMD from more ordered bilayer regions.

Materials and Methods

Liposome Preparation. Lipids were purchased from Avanti Polar Lipids. Solutions were prepared with Milli-Q purified type I H_2O. Eight micromoles of total lipids, i.e., POPC mixed or not with different proportions of a second lipid [CER, distearoyl-phosphatidylserine (DSPS), distearoyl-phosphatidylcholine (DSPC), or palmitoyl-oleyl-phosphatidylserine (POPS)], and with tritiated phosphatidylcholine (Amersham Pharmacia Biosciences) added as a tracer (300,000 dpm, corresponding to less than 0.0001% of total lipids), were dried under a stream of nitrogen from chloroform/methanol 2:1 (vol/vol) solutions and then under a vacuum for at least 3 h. After resuspension of the dried lipid film in 1 ml of 4 mM Tris·HCl, pH 7.4/400 mM KCl (Tris·KCl solution) plus 30 mM N-octyl glucoside (OG), liposomes were produced by dialysis at 37°C (molecular weight cutoff 6,000–8,000) against 3 1 liter of detergent-free Tris·KCl solution for 24 h. To obtain proteoliposomes, the bacterially expressed, purified $b_5$wt or $b_5$ext dissolved in 15–150 μl of PBS/30 mM OG were added to the lipid-detergent solution in 1:500 molar ratio to the lipids unless otherwise specified. The protein-lipid detergent mixture was then dialyzed as above. The recovery of lipids after dialysis, determined by liquid scintillation counting of the tracer and by TLC, was 60–80%; the two lipids in binary mixtures were recovered with equal efficiency. Protein recovery, estimated by SDS/PAGE, was in the same range as that of lipids.

Characterization of Liposomes. *Gel filtration.* Suspensions of proteoliposomes containing either $b_5$wt or $b_5$ext were loaded on a 0.8 cm 16.5 cm column of Sepharose CL-4B or CL-2B, respectively, equilibrated in Tris·KCl solution. Fractions (0.4 ml) were collected, of which an aliquot was counted in a β-counter to reveal the presence of the radioactive lipid tracer. The fractions were then pooled two by two, and equal aliquots were analyzed by Western blot-enhanced chemiluminescence (Pierce, pico system) with anti-cytochrome b_5 antibodies (15).

Carbonate extraction and flotation. Two hundred-microliter aliquots of liposomes containing one of the b_5 forms were treated with an equal volume of 0.2 M Na_2CO_3 for 30 min on ice and then brought to 1.2 M sucrose 0.1 M Na_2CO_3 in a final volume of 1 ml. The samples were layered under discontinuous sucrose gradients composed of layers (1, 0.5, 0.25, 0.15, and 0 M sucrose all containing 0.1 M Na_2CO_3), 0.8 ml each, which were centrifuged overnight at 40,000 rpm at 4°C (Beckman SW 55 rotor). One-milliliter fractions were TCA-precipitated and then analyzed by SDS/PAGE.

DSC. Calorimetric analysis was performed with MC-2D or VP-DSC high sensitivity differential scanning calorimeters (Microcal, Amherst, MA) interfaced to a personal computer for automatic data collection and analysis. The calorimetric scans were performed at a rate of 20°C/h starting from 4°C. In all of the figures, the data have been normalized to 1 μmol of total lipids.

Curve fitting, based on nonlinear-least-squares minimization (Microcal DECONV program) was used to estimate the T_m and the enthalpy change (H) associated with the transition of the components when the thermogram was the summation of overlapping peaks. The deconvolution is based on the assumption that the thermograms are the result of a linear combination of more than one independent two-state transitions (16). Summation of the deconvolved components yielded theoretical curves whose standard deviation from the experimental ones never exceeded 0.04 mcal·°C $^{1}\cdot\mu$mol ^{1}.

Fluorescence Excimer Formation Measurements. The probes used were 1-palmitoyl-2-(1-pyrenedecanoyl)-sn-glycero-3-phosphocholine (pyrene-PC, Molecular Probes, Eugene, OR) and 1-palmitoyl-2-(1-pyrenedecanoyl)-sn-glycero-3-phosphoserine (pyrene-PS, a kind gift of P. Somerharju, University of Helsinki, Helsinki). Liposomes or proteoliposomes containing one of the two probes were produced by dialysis from OG-containing solutions as described under Liposome Preparation The excimer/monomer intensity ratio of the probe-containing liposomes was determined by using a Cary Eclipse spectrofluorimeter (Varian), exciting at 342 nm, and reading at 398 (monomer) and 480 nm (excimer).

Supporting Information. Purification of the two b_5 forms and electron microscopy are described in Supporting Text which is published as supporting information on the PNAS web site.

Results

Reconstitution of $b_5$wt or $b_5$ext into Liposomes. The two b_5 proteins, which differ only in TMD length and that were used for our studies (represented in Fig. 1A), were cleaved from the corresponding GST fusion proteins isolated from bacterial lysates (Fig. 7A, which is published as supporting information on the PNAS web site). To reconstitute the proteins into liposomes, the detergent dialysis method, which is thought to ensure true integration of the TMD of b_5 into the phospholipid bilayer (17) was chosen. As a constituent of the liposome bilayer matrix, we used POPC, a phospholipid with a low T_m that is abundant in eukaryotic cells (18) and well represented also in the ER (3). A second lipid, with a higher T_m, was included in binary mixtures. This lipid was either a glycerophospholipid differing from POPC in its acyl chains and/or headgroup (DSPC, DSPS, or POPS) or a sphingolipid (CER). Dialysis from OG-containing solutions allowed quantitative integration of the two b_5 forms into these different liposomes, as assessed by gel filtration. Indeed, as illustrated for DSPS proteoliposomes (Fig. 1B), the two proteins were quantitatively recovered in the void volume of Sepharose columns together with the lipids, in fractions well separated from those containing the proteins processed in parallel in the absence of lipids. Identical results were obtained for all of the proteoliposome preparations used in our experiments. Moreover, the proteins were tightly integrated into the lipid bilayer, as demonstrated by their resistance to extraction by treatment with 0.1 M Na_2CO_3 and subsequent flotation on alkaline sucrose gradients (illustrated in Fig. 1C for POPC/CER 9:1 proteoliposomes). The liposomes were also analyzed by negative staining. In all cases, we observed vesicles within the expected size range (50–100 nm) and incorporation of b_5 proteins did not noticeably alter the appearance of the liposomes (Fig. 7B).

DSC Analysis. *POPC.* We first analyzed liposomes composed only of POPC, in the presence or absence of protein. As shown in Fig. 2 Aa and B, the excess heat capacity vs. temperature plot of pure POPC liposomes exhibits the presence of an endothermic transition, centered at 3.4°C, corresponding to the T_m of the lipid, with an associated enthalpy (H) of 3.22 kcal/mol. Insertion of $b_5$wt (Fig. 2 Ab) or $b_5$ext (Fig. 2 Ac) in the liposome bilayer caused a significant and comparable decrease (16%) in the H with no significant modification of the T_m (Fig. 2B).

POPC/POPS. Phosphatidylserine (PS) is at least three times more concentrated in the plasma membrane than in the ER, its site of synthesis (4), and acidic phospholipids appear to be required for formation of transport vesicles exiting the ER (19, 20). There-

Fig. 1. Characterization of liposomes containing b 5wt or b 5ext. (A) Schematic representation of the b 5 forms used in our studies. The gray ovals represent the cytosolic catalytic domain of cyt b 5, the underlined residues constitute the predicted TMD of 17 amino acids (15), and those shown in enlarged bold were added to form the lengthened TMD (22residues) of b 5ext. (B and C) b5wt and b 5ext are quantitatively integrated into liposomes by the detergent dialysis method. (B) Gel ltration analysis of 0.9:0.1 POPC /DSPS proteoliposomes with embedded b 5wt (Left) or b 5ext (Right). The lower graphs show the elution pro le of the radioactive lipid tracer. Fractions 8 and 9 correspond to the void volume. The Western blot analyses shown above the radioactivity pro le reveal that both proteins are quantitatively recovered with the liposomes. The upper Western blots show the elution pro le for the two proteins subjected to dialysis from OG solution but without the addition of lipids. (C) Resistance to alkaline extraction of b 5wt and b 5ext incorporated into liposomes. 0.9:0.1 POPC /CER proteoliposomes with incorporated b 5wt or b 5ext were treated with Na 2CO3 and analyzed by otation on sucrose gradients. The Coomassie-stained gels of the fractions collected from the gradients are shown. Fraction 2 (loaded in lane 2 in both images) contains the 0.15M /0.25M sucrose interface. The arrow on the left indicates the position of the 21-kDa size marker.

fore, we analyzed the behavior of the two differently sorted b_5 forms in binary POPC/POPS mixtures. First, we determined the thermotropic parameters of protein-free vesicles made with different proportions of the two lipids. In accordance with other DSC studies on PS (21), the negatively charged headgroup of POPS caused a T_m increase of nearly 18°C compared with POPC (Fig. 8, which is published as supporting information on the PNAS web site). Consistently, in binary POPC/POPS mixtures an additional peak was present on the high temperature side of the gel-liquid phase transition of POPC, indicating that at least two phases were coexisting. The thermograms could be best fit by two components by deconvolution analysis. Such analyses showed that, with increasing POPS molar fraction (χ_{POPS}), the amplitude of the higher temperature melting component increased at the expense of the lower melting component (Fig. 8). The higher temperature melting component showed a relative contribution to the total enthalpy larger than expected on the basis of the POPS proportion in the bilayer, suggesting its correspondence with a POPS-enriched, POPS/POPC domain.

Incorporation of $b_5$wt or $b_5$ext into POPC/POPS (9:1, M:M) liposomes had marked but opposite effects on the thermotropic properties of the bilayer (Fig. 3A b and c). Insertion of $b_5$wt decreased the relative contribution of the lower T_m component (mainly constituted by POPC) to the total H from 60% to 33%; in contrast, $b_5$ext decreased the contribution of the higher T_m component, corresponding to the DSPS-rich domain, from 40% to 34% (Fig. 3B). Because the only structural difference between the two b_5 constructs is in the TMD, the different effects of the two proteins on the thermotropic properties of liposomes were likely due to different partitioning into lipid domains.

POPC–DSPC Because disaturated glycerophospholipids are more abundant at the plasma membrane than in the ER and are thought to be preferentially transported from the ER to the cell surface (3, 4), we investigated the effects of the two b_5 constructs on the thermotropic properties of binary mixtures of POPC with a disaturated glycerphospholipid carrying the same phosphocholine headgroup (DSPC). The addition of DSPC, at any proportion, caused the appearance of a second peak, separated from the main POPC transition; the T_m and H of the second peak increased with increasing χ_{DSPC} (Fig. 9, which is published as supporting information on the PNAS web site), suggesting its identity with a DSPC-enriched domain.

Fig. 2. Excess heat capacity vs. temperature plots of POPC liposomes with or without integrated b 5 forms. (A) Representative scans of liposomes in the absence of integrated protein (a) or with integrated b 5wt (b) or b 5ext (c), with a protein:lipid molar ratio of 1:1,000. (B) Mean values for T_m and H for the gel-liquid transition SEM (n 3) for pure POPC vesicles or POPC proteoliposomes containing b 5wt or b 5ext.

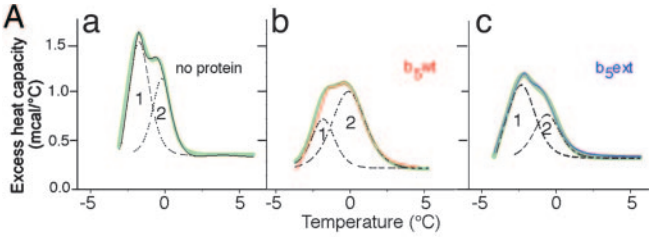

B

	T_m 1 (°C)	T_m 2 (°C)	% ΔH in peak 2 (kcal/mol)
no protein	-1.81 ± 0.1	-0.80 ± 0.03	39.9 ± 1.3 1.34 ± 0.03
$b_5$wt	-1.48 ± 0.04	-0.21 ± 0.01	66.5 ± 2.8** (2.0 ± 0.05)
$b_5$ext	-1.53 ± 0.4	-0.63 ± 0.03	33.9 ± 1.1** (0.92 ± 0.04)

Fig. 3. Excess heat capacity vs. temperature plots of POPC /POPS liposomes (9:1, M:M) with or without integrated b 5 forms. (A) Representative scans of liposomes in the absence of integrated protein (a) or with integrated b 5wt (b) or b 5ext (c). The dashed lines indicate the two component peaks obtained by deconvolution analysis. The experimental curves are shown in black, red, or blue for protein-free, b 5wt, and b 5ext, respectively. The thick light green line shows the theoretical curve resulting from the summation of the two components resolved by deconvolution analysis. (B) Mean values SEM (n 3) of T_m for components 1 and 2 indicated in A and H and % contribution to total H of component 2. **, P 0.01 by Student's t test for % H of component 2 in b 5wt vs. b 5ext proteoliposomes.

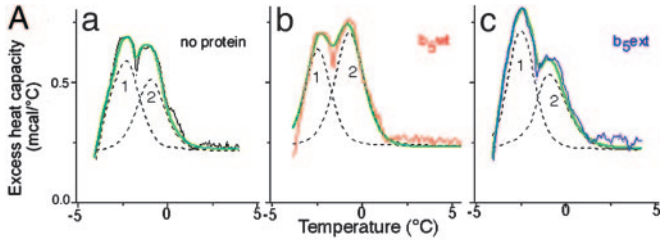

B

	T_m 1 (°C)	T_m 2 (°C)	% ΔH in peak 2 (kcal/mol)
no protein	-2,42 ± 0.10	-0.95 ± 0.03	52.3 ± 1.5 (1.02 ± 0.11)
$b_5$wt	-2,45 ± 0.05	-0.94 ± 0.06	58.3 ± 1.3** (1.18 ± 0.08)
$b_5$ext	-2.43 ± 0.05	-1.01 ± 0.05	41.3 ± 2.0** (0.90 ± 0.14)

Fig. 5. Excess heat capacity vs. temperature plots of (9:1, M:M) liposomes with or without integrated b 5 forms. (A) Representative scans of liposomes in the absence of integrated protein (a) or with integrated b 5wt (b) or b 5ext (c). (B) Mean values of thermotropic parameters obtained from three experiments. Symbols and color coding are as in Fig. 3.

As shown in Fig. 4, the effects of the two b_5 constructs inserted into 0.9:0.1 POPC/DSPC liposomes were indistinguishable. Remarkably, no difference in the amplitude and T_m of the higher temperature, DSPC-rich domain was induced by either of the two proteins, although each one produced a significant and comparable increase in the enthalpy of the main POPC transition.

*POPC/DSPS*PS species at the plasma membrane are particularly enriched in unsaturated fatty acyl chains compared with the ER (22). Therefore, we completed our investigation on binary glycerophospholipid mixtures by analyzing POPC/DSPS liposomes. The thermotropic behavior of these liposomes was quite similar to that of POPC/POPS liposomes (Fig. 10, which is published as supporting information on the PNAS web site vs.

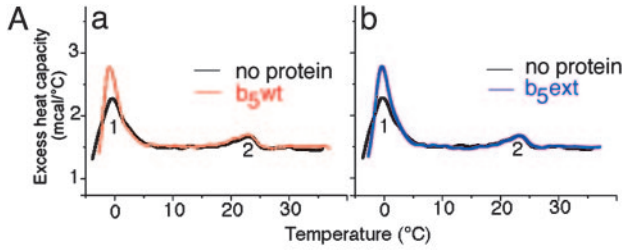

B

	T_m 1 (°C)	T_m 2 (°C)	% ΔH in peak 2 (kcal/mol)
no protein	-0.43± 0.02	23.06 ± 0.05	22.04 ± 1.2 (1.06 ± 0.09)
$b_5$wt	-0.88 ± 0.04	23.06 ± 0.05	14.2 ± 2.4 (1.05 ± 0.10)
$b_5$ext	-0.88 ±0.03	23.24 ± 0.04	13.8 ± 3.2 (1.07± 0.14)

Fig. 4. Excess heat capacity vs. temperature plots of POPC /DSPC (9:1, M:M) liposomes with or without integrated b 5 forms. (A) Representative scans of liposomes in the absence of integrated protein (black trace in a and b) or with integrated b 5wt (red trace in a) or b 5ext (blue trace in b). (B) Mean values SEM. (n 3) of T_m for components 1 and 2 indicated in A and of H and % contribution to total H of component 2.

Fig. 8), at least up to 0.6 χ_{DSPS}, with the presence of a shoulder or a partially overlapping but distinguishable second peak at the high temperature side of the main POPC transition.

The behavior of the two b_5 forms in POPC/DSPS (9:1, M:M) liposomes was qualitatively similar to the one observed in POPC/POPS mixtures, i.e., $b_5$wt increased and $b_5$ext decreased the relative contribution of the higher melting, DSPS-enriched component to the total H (Fig. 5 A and B). This observation again suggests a different partitioning of the two proteins into lipid domains.

*POPC-ceramide*We next investigated POPC liposomes containing CER, a sphingolipid that is synthesized in the ER but then exported to the Golgi complex (4). Representative DSC scans for POPC/CER binary mixtures are illustrated in Fig. 6 (see also Fig. 11, which is published as supporting information on the PNAS web site). Low proportions (5%) of CER caused the appearance of a shoulder on the high temperature side of the main POPC transition. The composite peak could be best fit by two components by deconvolution analysis, suggesting that part of the POPC molecules shift from a lower T_m, POPC phase to a phase-separated, higher temperature melting, CER-enriched domain (Fig. 11). Concomitantly, with increasing χ_{CER}, a third, high melting component appeared, increasing in amplitude and moving toward the T_m of pure CER (Fig. 11).

As shown in Fig. 6, and analogously to our observations on POPC/PS mixtures, $b_5$wt and $b_5$ext affected the POPC/CER liposomes in opposite ways, in that the relative contribution to the total H of the low T_m, POPC-enriched component decreased from 76% to 61% after $b_5$wt insertion. In contrast, $b_5$ext caused a decrease of the relative contribution of the higher T_m, CER-containing, minor component from 24% to 10% (Fig. 6B). Noticeably, $b_5$ext insertion also caused a downward shift in the T_m of the lower temperature melting, major domain. These results suggest that $b_5$ext but not $b_5$wt was removing CER molecules from the gel to liquid crystalline phase transition.

Fluorescence Studies.To confirm the different interaction of the two b_5 forms with lipid domains, we applied an alternative method, based on fluorescence measurements of excimer formation coupled to the use of the pyrene-labeled fluorescent probes pyrene-PS or pyrene-PC inserted in POPC liposomes. Changes in excimer/monomer intensity ratios induced by associated proteins can give information on the interactions of the

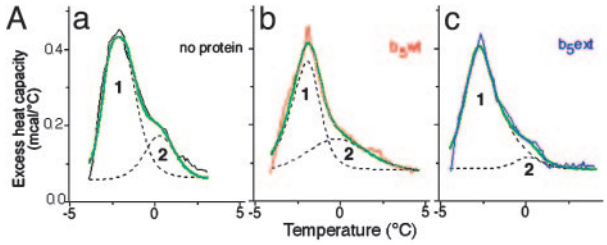

B

	T_m 1 (°C)	T_m 2 (°C)	% ΔH in peak 2 (kcal/mol)
no protein	-2.23 ± 0.09	0.036 ± 0.07	24.2 ± 5.7 (0.26 ± 0.05)
$b_5$wt	-2.00 ± 0.06	-0.151 ± 0.07	39.1 ± 5.0* (0.42 ± 0.06)
$b_5$ext	-2.74 ± 0.05	0.166 ± 0.1	9.5 ± 1.5* (0.09 ±0.01)

Fig. 6. Excess heat capacity vs. temperature plots of POPC /CER (9:1, M:M) liposomes with or without integrated b 5 forms. (A) Representative scans of liposomes in the absence of integrated protein (a) or with integrated b 5wt (b) or b 5ext (c). (B) Mean values of thermotropic parameters obtained from three experiments. Symbols and color coding are as in Fig. 3. *, P 0.05 by Student's t test for % H of component 2 in b 5wt vs. b 5ext proteoliposomes.

proteins with the lipid probes or with the lipid domains that contain them (23).

As shown in Table 1, the fluorescence spectroscopy measurements showed that the excimer/monomer intensity ratio of pyrene-PS increased (17.5%) in liposomes containing $b_5$ext with respect to control liposomes but did not change in the presence of $b_5$wt. These data, in addition to confirming the different behavior of the two proteins toward PS observed by DSC, suggest that $b_5$ext may interact with pyrene-PS, inducing its recruitment to the neighborhood of the protein. Differently from pyrene-PS, pyrene-PC fluorescence was unaffected by incorporation of either b_5 form, thus confirming the DSC results.

Discussion

In recent years, increasing attention has been directed to lipid–protein interactions, which have been implicated in important cellular functions such as signal transduction, cell adhesion and motility, and protein sorting within the secretory pathway. Studies in epithelial cells have led to the hypothesis that lipid microdomains enriched in sphingolipids and cholesterol (rafts) within the trans-Golgi network serve as platforms for delivery of membrane proteins to the apical surface (24).

An important question is whether a similar lipid-based mechanism operates also at the early steps of the secretory pathway, namely at the ER/Golgi interface. There is very little information, however, on this problem, and evidence for the presence of lipid rafts within the ER membrane of mammalian cells is lacking. Indeed, presumably because of the absence in the ER of sphingomyelin and glycosphingolipids and because of its low cholesterol content (4, 25), detergent-resistant membranes have not been isolated from the mammalian ER. Of course, the detergent sensitivity of ER membranes does not rule out the possible existence of lipid domains within this compartment. Therefore, additional strategies, alternative to the use of detergents, should be sought to understand the role of lipid–protein interactions in protein sorting at the level of ER.

Table 1. Excimer/monomer ratio of uorescent probes in POPC liposomes with or without b 5 proteins

Protein	Pyrene-PC*		Pyrene-PS†	
None	0.100	0.002	0.120	0.004
$b_5$wt ‡	0.102	0.001	0.116	0.008§
$b_5$ext ‡	0.102	0.002	0.141	0.005§

*Molar ratio of Pyrene-PC to POPC was 1:99.
†Molar ratio of Pyrene-PS to POPC was 0.5:99.5.
‡Molar ratio of protein to phospholipids was 1:100.
§P for b 5wt versus b 5ext 0.002 by Student's t test.

Artificial membranes provide useful systems for the investigation of protein–lipid interactions, which are more easily recognized in this simplified context than in the complex environment of natural membranes. In the present study, we used liposomes composed of binary mixtures to probe for differences in interactions with lipids of two differently sorted TA proteins, the naturally occurring cytochrome b_5 ($b_5$wt), a resident of the ER, and a mutant form thereof, $b_5$ext, which, because of the presence of an additional five hydrophobic amino acids in its TMD, escapes from the ER to reach the plasma membrane (15). Apart from this difference, the two proteins are identical and, thus, provide useful tools for the analysis of the role of specific features of the TMD in protein–lipid interactions. For our investigation, we used high sensitivity DSC, because this technique, relying on physicochemical features of natural lipids, can reveal the occurrence of lipid phase separations and, at the same time, lipid–protein interactions within these phases (16). POPC was chosen as the constituent of the bulk lipid matrix, because on the one hand, it is homogeneously distributed among cellular membranes (3, 25) and is thus not expected to undergo sorting events, and, on the other hand, POPC liposomes are amenable to DSC analysis.

DSC analysis of POPC proteoliposomes containing $b_5$wt or $b_5$ext yielded identical thermograms, ruling out differences between the two proteins in their interaction with the POPC matrix. Both proteins decreased the enthalpy of the gel to liquid-crystalline transition of the lipid vesicles, most likely reflecting the decreased number of POPC molecules undergoing the gel-liquid transition consequent to the insertion of the TMD into the nonpolar core of the bilayer (reviewed in ref. 13).

We selected three different glycerophospholipids differing in acyl chains and/or headgroup and one sphingolipid (CER) for inclusion in binary mixtures with POPC. This choice was based on the consideration that these lipids, because they are synthesized in the ER but enriched in the plasma membrane (4, 25), are likely to be selectively transported out of the ER and/or excluded from vesicles directed back to this compartment by retrograde traffic.

Each of the four lipids in the bilayer caused the appearance of a second thermotropic transition at a higher temperature besides that of POPC, either displayed as an evident separated peak or as a shoulder on the high-temperature side of the POPC transition, suggesting that lateral phase separation was present. When the effects of $b_5$wt or $b_5$ext on the thermotropic properties of these mixed liposomes were analyzed, no differences were observed in the case of POPC/DSPC liposomes, and the DSPC-enriched domain was not affected by either of the two proteins. In contrast, in POPC/PS and POPC/CER liposomes, the two proteins had markedly different and opposite effects on the lower T_m (POPC-based) and higher T_m (PS- or CER-enriched) domains. The different effects of the two proteins on PS-containing bilayers was confirmed by an alternative technique, based on fluorescence measurements of lipid probes. These results indicate that the addition of five hydrophobic amino acids to the TMD of a TA protein can profoundly affect its interaction with lipids.

An interpretation in molecular terms of our observations must remain tentative, because it is known that different integral membrane proteins have widely differing effects on the thermotropic properties of artificial membranes, and that these differences are often difficult to explain (13). Keeping in mind

these limitations, the ability of $b_5$ext to cause a relative decrease of the higher melting component in POPC/PS and POPC/CER liposomes, can be nicely explained if one assumes preferential partitioning of the protein into this domain as a consequence of the higher hydrophobicity of its extended TMD. This positioning would result in the sequestration of lipid molecules (either PS or CER) from the cooperative transition. Similarly, preferentially partitioning of $b_5$wt into the more fluid POPC phase would explain its effect on the lower temperature melting component of the thermograms.

We also suggest an explanation for the lack of effect of $b_5$ext on the DSPC-enriched domain in POPC/DSPC liposomes. This component showed a much higher T_m and a much lower relative contribution to the total H than DS-separated domains. Because the amplitude of the phase separated peaks in DSC scans is related to the number of molecules undergoing the transition, and a higher T_m reflects a higher degree of packing of the fatty acyl chains (26), the main difference between PS-enriched and DSPC-enriched domains is likely attributable to the higher degree of intermixing of the PS with POPC. Both POPS and DSPS would be contained in loosely packed domains carrying a relevant POPC proportion, whereas DSPC would be more highly enriched in tightly packed domains carrying a low POPC proportion. It is plausible that there is an upper limit to the degree of order of lipid domains into which $b_5$ext preferentially partitions and that the DSPC-enriched domain exceeds this limit, explaining why the behavior of $b_5$ext in POPC/DSPC mixtures was indistinguishable from that of the wt protein. This interpretation is consistent with our previous observation that a plasma membrane localized reporter construct bearing the TMD of $b_5$ext was not recovered in cold detergent-resistant membrane fractions thought to contain liquid-ordered domains of the plasma membrane (27). Obviously, alternative hypotheses, based for instance on the capacity of PS and ceramide to form hydrogen bonds, cannot be discarded on the basis of the present study, and further work will be required to define the molecular basis of the different interaction of the two proteins with lipid domains.

We believe that the observations reported in this study may be relevant to lipid-based sorting mechanisms operating at the ER/Golgi interface. Clearly, in our model system, PS and CER were present in a higher concentration than in ER membranes (4). However, lipid–protein interactions occurring in the ER could facilitate concentration of certain lipids in ER subdomains, which would reciprocally affect protein distribution. Of particular relevance to our results is the observation that PS is enriched in transport vesicles generated in an in vitro budding reaction relative to the starting microsomes (6, 28). Another relevant observation is that acidic phospholipids such as PS are required for the generation of ER-like (COPII-coated) transport vesicles in a reconstituted system (19). Thus, it is tempting to speculate that saturated fatty acid-bearing acidic phospholipids are concentrated at the site of bud formation and, thereby, facilitate recruitment of cargo membrane proteins that preferentially interact with them, and excluding those destined for retention in the ER. As far as CER is concerned, recent work has demonstrated that its export from the ER to the site of sphingomyelin synthesis in the Golgi complex is mediated by the ceramide transfer protein CERT (29); however, a vesicular transport pathway is thought to coexist with this mechanism (30). Moreover, lipid sorting presumably occurs not only in anterograde but also in retrograde transport pathways (31). Thus, it could influence protein sorting at the ER/Golgi interface both at the exit and at retrieval steps.

In our previous studies, we demonstrated that a plasma membrane localized GFP construct that carries b_5 ext's tail is not associated with detergent-resistant membranes (27). In the present work, we have used a different approach, enabling us to probe for interactions of proteins with lipid domains that melt at low temperature. In this way, we reveal clear differences between the behavior of an exported and an ER-resident TA protein, suggesting an involvement of such interactions in sorting at the ER/Golgi interface. An extension of these studies with model systems should help to unravel protein–lipid interactions at the basis of sorting at the ER/Golgi interface.

We thank Teresa Sprocati and Silvia Sesana for technical assistance and for general helpfulness in the laboratory and P. Somerharju for his gift of pyrene-PS and for helpful suggestions. This work was supported by Italian Ministry of Research Grants PRIN-COFIN 2003 (to N.B.) and FIRB-COFIN 2003 (to M.M.) and Telethon Foundation Grant GGP04129 (to N.B.).

1. Lee, M. C., Miller, E. A., Goldberg, J., Orci, L. & Schekman, R. (2004) Annu. Rev. Cell Dev. Biol **20,** 87–123.
2. Bretscher, M. S. & Munro, S. (1993) Science **261,** 1280–1281.
3. Schneiter, R., Brügger, B., Sandhoff, R., Zellnig, G., Leber, A., Lampl, M., Athenstaedt, K., Hrastnik, C., Eder, S., Daum, G., et al. (1999) J. Cell. Biol. **146,** 741–754.
4. van Meer, G. (1989) Annu. Rev. Cell Biol. **5,** 247–275.
5. Nickel, W., Bruegger, B. & Wieland, F. T. (1998) Semin. Cell Dev. Biol. **9,** 493–501.
6. Sturbois-Balcerzak, B., Vincent, P., Maneta-Peyret, L., Duvert, M., Satiat-Jeunemaitre, B., Cassagne, C. & Moreau, P. (1999) Plant Physiol. **120,** 245–256.
7. Brown, D. A. & Rose, J. K. (1992) Cell **68,** 533–544.
8. Scheiffele, P., Roth, M. G. & Simons, K. (1997) EMBO J. **16,** 5501–5508.
9. Horvath, A., Suetterlin, C., Manning-Krieg, U., Movva, N. R. & Riezman, H. (1994) EMBO J. **13,** 3687–3695.
10. Borgese, N., Colombo, S. & Pedrazzini, E. (2003) J. Cell Biol. **161,** 1013–1019.
11. Sato, K., Sato, M. & Nakano, A. (2003) Mol. Biol. Cell **14,** 3605–3616.
12. Rayner, J. C. & Pelham, H. R. B. (1997) EMBO J. **16,** 1832–1841.
13. McElhaney, R. N. (1986) Biochim. Biophys. Acta **864,** 361–421.
14. Terzaghi, A., Tettamanti, G. & Masserini, M. (1993) Biochemistry **32,** 9722–9725.
15. Pedrazzini, E., Villa, A. & Borgese, N. (1996) Proc. Natl. Acad. Sci. USA **93,** 4207–4212.
16. Ferraretto, A., Pitto, M., Palestini, P. & Masserini, M. (1997) Biochemistry **36,** 9232–9236.
17. Takagaki, Y., Radhakrishnan, R., Wirtz, K. W. A. & Khorana, H. G. (1983) J. Biol. Chem. **258,** 9136–9142.
18. Ekroos, K., Ejsing, C. S., Bahr, U., Karas, M., Simons, K. & Shevchenko, A. (2003) J. Lipid Res. **44,** 2181–2192.
19. Matsuoka, K., Orci, L., Amherdt, M., Bednarek, S. Y., Hamamoto, S., Schekman, R. & Yeung, T. (1998) Cell **93,** 263–275.
20. Pathre, P., Shome, K., Blumental-Perry, A., Bielli, A., Haney, C. J., Alber, S., Watkins, S. C., Romero, G. & Aridor, M. (2003) EMBO J. **22,** 4059–4069.
21. Mattai, J., Hauser, H., Demel, R. A. & Shipley, G. G. (1989) Biochemistry **28,** 2322–2330.
22. Keenan, T. W. & Morré, D. J. (1970) Biochemistry **9,** 1277–1283.
23. Junker, M. & Creutz, C. E. (1993) Biochemistry **32,** 9968–9974.
24. Simons, K. & Ikonen, E. (1997) Nature **387,** 569–572.
25. Colbeau, A., Nachbaur, J. & Vignais, P. M. (1971) Biochem. Biophys. Acta **249,** 462–492.
26. Huang, C.-h. & Li, S. (1999) Biochim. Biophys. Acta **1422,** 273–307.
27. Bulbarelli, A., Sprocati, T., Barberi, M., Pedrazzini, E. & Borgese, N. (2002) J. Cell Sci. **115,** 1689–1702.
28. Moreau, P., Cassagne, C., Keenan, T. W. & Morré, D. J. (1993) Biochim. Biophys. Acta **1146,** 9–16.
29. Hanada, K., Kumagai, K., Yasuda, S., Miura, Y., Kawano, M., Fukasawa, M. & Nishijima, M. (2003) Nature **426,** 803–809.
30. Fukasawa, M., Nishijima, M. & Hanada, K. (1999) J. Cell Biol. **144,** 673–685.
31. Brugger, B., Sandhoff, R., Wegenhingel, S., Gorgas, K., Malsam, J., Helms, J. B., Lehmann, W. D., Nickel, W. & Wieland, F. T. (2000) J. Cell Biol. **151,** 507–518.